Models of settling lag in coastal and estuarine settings

David Pritchard[1] and Andrew J. Hogg[2]

1. Introduction

The two principal processes driving coastal and estuarine sediment transport — tides and waves — are oscillatory flows which involve no net movement of water when averaged over the period of the fluid motion. It is well-known, however, that such flows can lead to the net movement of sediment in a particular direction. For sufficiently coarse sediment, the direction of net transport generally corresponds to the direction of peak current velocities, because of the non-linear dependence of bedload transport rate on velocity. For finer sediment, which is transported largely in suspension, the process depends more on "lag" effects associated with the finite time which it takes the quantity of sediment in suspension to adjust to changes in the fluid velocity. Especially when this response time is comparable to the period of the motion, the character of these lag effects can be rather complex, and is still less well understood than the processes leading to net bedload transport.

This paper draws on recent studies of fine sediment transport on muddy coasts by Pritchard & Hogg (2003a,b). In these studies, tidal currents and infragravity waves were considered as agents of sediment transport within a mathematical model: in this paper, we will compare four different oscillatory flows (two corresponding to tidal currents and two to infragravity waves), and discuss the net transport patterns which emerge.

1.1. Conceptual models of settling lag

The processes of settling lag and scour lag were proposed by van Straaten & Kuenen (1958) and by Postma (1961) to explain the accumulation of fine sediment in the landward reaches of tidal inlets. They are best understood when the hydrodynamics are considered in Lagrangian terms, following individual "fluid elements" within the flow. The basic mechanism of settling lag is that a suspended sedimentary particle takes a finite time to settle out of suspension, and thus is carried landwards on the flood (or run-up) some distance after the local fluid velocity has fallen below the threshold velocity for deposition. It is therefore re-entrained on the ebb (or run-down) not by the fluid element which deposited it, but by one located further landwards. Figure 1 illustrates some ways in which this process can lead to the net landwards movement of sediment. Particle deposition and re-entrainment by different fluid elements is further accentuated if the threshold velocity for the erosion of sediment, u_e, is higher than the threshold velocity for deposition u_d. This accentuation is known as scour lag: for simplicity, we neglect it in the following discussion.

Figure 1a shows the case where the hydrodynamics are spatially uniform. A particle is entrained on the "flood" (A) and carried until just before high water slack (HWS), when the current drops below the threshold for deposition; it then takes a finite time to settle from suspension, and reaches the bed (B) a distance Δ_{HW} beyond the point at which it started to settle. On the "ebb", the particle is re-entrained by an initially more landward fluid element, which carries it seawards until it starts to sink shortly before low water slack (LWS); finally, it is deposited again (C) a distance Δ_{LW} beyond where it started to sink. Since in this situation

[1] BP Institute for Multiphase Flow, University of Cambridge, Madingley Rise, Cambridge CB3 0EZ, England. E-mail: david@bpi.cam.ac.uk. Fax: +44 1223 765 701.
[2] Centre for Environmental and Geophysical Flows, Department of Mathematics, University of Bristol, University Walk, Bristol BS8 1TW, England. E-mail: a.j.hogg@bristol.ac.uk. Fax: +44 117 928 7999.

the trajectories of all fluid element are identical and the settling distances Δ_{HW} and Δ_{LW} are the same, the particle is re-deposited where it started off.

Figure 1b shows the case where fluid trajectories are identical, but the settling distance at HWS exceeds that at LWS (for example, because of differences in the depth of fluid). In this case, the particle is deposited further landwards than it started; similarly, if $\Delta_{HW} < \Delta_{LW}$ we may expect net seawards transport. Conversely, figure 1c shows a case where settling distances are identical, but the fluid trajectories are not. Here, the smaller excursion of the more landward fluid element means that the particle is deposited further landward than it started; similarly, if the excursion were greater for fluid elements located further landwards, the particle would be deposited further seawards than it started.

Van Straaten & Kuenen (1958) argued that in tidal inlets, the maximum velocity and tidal excursion of a fluid element increase seawards, so the mechanism illustrated in figure 1c leads to net landwards transport. This was questioned by Postma (1961), who argued that it was misleading to consider sediment dynamics in terms of individual particles, and that a continuum model should be employed to represent the stochastic nature of sediment response. The mechanism Postma proposed depends on an asymmetry in the hydrodynamics: typically fluid accelerations are lower around HWS than around LWS, leading to a longer period when sediment can be deposited, and thus to lower concentrations on the ebb than on the flood. As figure 1d illustrates, this cannot be explained in terms of a particulate model of sediment dynamics, because the settling distance of an individual particle does not depend on the length of slack water, and Postma also suggested that it was unlikely that the settling lag mechanisms proposed by van Straaten & Kuenen could be identified in a continuum model.

More recent conceptual treatments of settling lag employ a modified version of van Straaten & Keunen's mechanism, where the idea of the particulate settling time is replaced by the more general notion of the time taken for the concentration field to respond to changes in the fluid velocity, and in many estuarine contexts the processes leading to a net landwards movement of sediment can be described in these terms. Meanwhile, however, the principal tools for the simulation of sediment transport employ continuum models, which describe the fluid and sediment dynamics in terms of the fluid depth h and the vertically averaged fluid velocity u and mass concentration c of suspended sediment. (The key diagnostic quantities in these models are then the instantaneous cross-shore flux of sediment, $q(x,t) = cuh$, and the net flux $Q(x)$ obtained by integrating q over a period of the fluid motion.)

Although Postma's settling lag mechanism was first demonstrated in a continuum model by Groen (1967), comparatively few other analytical studies have considered net transport processes in the light of lag effects. In this paper, we will investigate how the particulate description may be of use in understanding the predictions of such models, with the aim of helping bridge the gap between the most ubiquitous mathematical and conceptual descriptions of fine sediment transport, and establishing the various rôles which lag effects may play.

2. Tidal flow across mudflats

We first consider the transport patterns under cross-shore tidal currents on an intertidal flat. We will consider two bathymetries: firstly, a linear flat with constant gradient, and secondly, the "morphodynamic equilibrium" flat proposed by Friedrichs & Aubrey (1996), which is linear below mean sea level and convex above. In each case, the forcing tide leads to a sinusoidal variation in surface elevation across the flat.

2.1. Transport across a linear flat

In tidal flow over a linear flat, the trajectories of all fluid elements are identical apart from translation (figure 2), and the durations of HWS and LWS are also identical. However, the fluid element which carries a particle on the ebb tide is located further landwards than that which carries it on the flood tide; hence the fluid depth is smaller, the particle takes less time to settle out around LWS, and $\Delta_{HW} < \Delta_{LW}$, leading to net landwards transport.

It is also informative to consider this process in Eulerian terms. The instantaneous depth-integrated sediment fluxes $q(x,t)$ at several points across a linear flat are shown in figure 3a, and the net flux $Q(x)$ integrated over a tide is shown in figure 3b. In a Lagrangian frame, the suspended sediment concentration (SSC) varies periodically with half the period of the fluid motion, and so the lag of the concentration field behind the velocity field must be identical on the flood and on the ebb. However, in the Eulerian frame, because the sediment-laden region is advected backwards and forwards the phase relation is correspondingly advanced or retarded, and so the fluxes become asymmetrical and need not cancel out when integrated over a tidal cycle.

Even at points below low water where there is a net balance between seawards and landwards fluxes, the sediment flux is far from symmetrical between flood and ebb. The flood is associated with a higher peak flux, but because it occurs when the fluid velocity is already falling and as lower concentrations are being advected landwards from the offshore region, it is shorter-lived; whereas the peak on the ebb occurs slightly before maximum ebb velocity, and so although it is lower, it is sustained for longer by the entrainment of sediment and by the seawards advection of the high concentrations associated with the turbid tidal edge. In the intertidal region, the sediment flux is still more weakly correlated with the instantaneous velocity, and this is particularly noticeably on the upper flat on the ebb (compare the times at which the local minimum of q occurs for the values of x plotted in figure 3a).

The phase lag between SSC and fluid velocity is the Eulerian “signature” of the settling lag process described in section 1.1. It occurs essentially because the dynamics of suspended matter are naturally Lagrangian in character, while sediment exchanges with the bed must be considered in an Eulerian frame. When a particle is deposited and re-entrained, it changes its position in the Lagrangian but not in the Eulerian frame, and thus lags behind the velocity field, which follows the Lagrangian co-ordinate; correspondingly, a phase lag in the Eulerian frame corresponds to the transfer of material between fluid elements in the Lagrangian frame.

So far the picture of settling lag which emerges from a continuum model is reasonably simple. However, it takes only a small change to the hydrodynamics to alter the picture noticeably.

2.2. Transport across a linear-convex flat

In tidal flow over a linear-convex flat, the transport mechanisms become more complicated, and the interpretation in terms of a particulate model of settling lag can be misleading. The convex bathymetry means that tidal excursion increases landwards (figure 4a), promoting the export of sediment. It also means that fluid depths are generally lower around HWS, and the higher velocities on the upper flat reduce the duration of HWS, decreasing Δ_{HW} relative to Δ_{LW}, which should further accentuate this effect. In this light, the landwards net transport evident on the upper flat (figure 4b) is at first puzzling.

However, when the process is considered in terms of a continuum model of sediment dynamics, a different picture emerges on the upper flat. Because of the smaller depths, a much greater quantity of sediment is able to deposit at HWS than at LWS, leading to lower concentrations at the start of the ebb than at the start of the flood, and thus to a net landward flux of sediment. This effect is most significant in shallow water, where the proportional difference in fluid depth caused by the convex bathymetry is greatest. Consequently, on the upper flat, this latter mechanism is dominant, leading to the net landwards transport of sediment; further seawards, however, lag effects associated with the difference in excursion start to dominate, and we see a small net seawards movement of sediment.

Far from the shore, interpretation in terms of individual particles again becomes difficult, because the water is sufficiently deep that typical settling times are comparable to the period of the fluid motion. The seaward transport here can best be explained by considering the behaviour of a fluid element far from the shore. In the absence of the convex upper flat, such an element would experience a variation in the forcing u^2 with twice the frequency of the tide, and correspondingly periodic sediment concentrations would result. However, the presence of the convex upper flat enhances velocities while it is inundated, thus suppressing deposition around HWS, and enhancing erosion during the end of the flood and the start of the ebb phases. The net result is that SSC is slightly higher on the ebb than on the flood, leading to a net seawards flux of suspended sediment.

The pattern of net sediment flux which emerges, then, is the result of various settling lag effects which compete to transport material landwards and seawards, with different mechanisms being dominant in different parts of the flat. This competition may lead to the emergence of equilibrium states of the morphodynamic system (see Pritchard & Hogg 2003a).

3. Infragravity waves on linear flats or beaches

As a third example, we consider the reflected long waves on a linear flat illustrated in figure 5a. The particle trajectories here are nearly sinusoidal, but the non-linear form of the oscillation means that fluid accelerations are slightly lower around maximum run-up than around maximum run-down. (This is most easily seen by comparing the shoreline in figure 5a with the sinusoidal curve of the same amplitude which is also plotted.)

Under these waves, the concentration field is spatially localised in a small region in and just seawards of the swash zone: further seawards, the fluid velocities are insufficient to suspend sediment. Settling lag is most easily visualised when the solution is displayed in Lagrangian form (figure 5b), where the delayed response of the SSC to changes in the velocity may be clearly seen. The lower accelerations around maximum run-up lead to a longer depositional period; consequently, sediment concentrations are generally a little lower during run-down: we may expect this to lead to the net movement of sediment up the flat, and this enhances the landward movement of sediment on the upper part of the flat.

Figure 6 illustrates the net cross-shore sediment flux $Q(x)$. In the upper part of the active region, corresponding roughly to the swash zone, there is a net shorewards movement of sediment, with deposition above about $x = 0.005$ and erosion below. The peak value of the net fluxes in this region is around 15% of the peak value of the instantaneous fluxes (omitted here for brevity), indicating the strong rôle which lag effects play in this region. In the lower part of the active region, the direction of net flux reverses, with material being eroded from around

the point of minimum shoreline penetration and deposited further seawards. This seawards flux gradually decays seawards until it reaches a point where there is no sediment mobilisation and consequently no net transport.

This net seawards movement of sediment occurs because of the lower concentrations which occur offshore: on the run-up, these low concentrations are advected landwards, so that even though sediment is being eroded, the peak flux on the run-up is slightly lower than that on the run-down in this region of the flat. This effect is rather weak, and in the upper part of the active region it is easily swamped by the shorewards transport due to settling lag, but in deeper regions, where Lagrangian concentrations vary less over a cycle and so lag effects are reduced, it makes its presence felt.

Finally, we consider a more complex bimodal infragravity oscillation, where the relative phase φ of the secondary frequency is varied so that the peak velocity under the wave is directed seawards or landwards. Figure 7a illustrates the near-shore hydrodynamics, and figure 7b shows the net sediment flux.

Compared to the monochromatic standing wave, two differences are evident. The first is the generally higher net flux, which occurs because the peak velocities which dominate sediment transport are higher under the bimodal wave. The second feature is that landwards transport in the swash zone and just offshore is substantially enhanced compared to the seawards transport which was evident for the monochromatic wave. This occurs because there is no longer a node of the velocity field just offshore, and so the ability of the low-velocity region to trap sediment through settling lag is much reduced.

The hydrodynamics for $\varphi = 0$ and $\varphi = \pi/2$ show an asymmetry in peak velocities, with the quantity u^2/u_e^2-1, which is proportional to the erosion rate, being up to 44% higher in one direction than the other. Since sediment transport is dominated by the peak velocities attained by the flow, this asymmetry might be expected to influence the net flux of sediment. Figure 7b, however, shows little sign of this, with the net fluxes for $\varphi = 0$ and $\varphi = \pi/2$ being comparable in the swash zone, and almost identical further offshore. The more substantial difference is between the net fluxes for $\varphi = \pi/4$ and $\varphi = 3\pi/4$: the former is considerably more strongly biased in favour of landwards transport even though they have identical maximum and minimum velocities. An explanation can be found in the sequence in which on- and offshore peak flows occur. The onshore peak in velocity for $\varphi = \pi/4$ is followed by a weaker offshore flow and then by a period of low onshore velocities, allowing the sediment mobilised around $t = 1$ to be carried landwards. The onshore peak in velocity for $\varphi = 3\pi/4$, on the other hand, is succeeded by a strong offshore flow, reducing the tendency of settling lag to move material landwards.

Overall, however, the most striking feature of figure 7b is that the general pattern of transport across the swash zone is almost identical in each case, further indicating the robustness of this pattern to the details of the hydrodynamics on the flat. In other words, the frequency spectrum of the wave forcing appears not to be crucial in determining the overall patter of sediment transport.

4. Discussion and conclusions

The results presented above illustrate the basic mechanism of settling lag, by which the finite response time of suspended sediment concentration translates into a phase lag between

velocity and suspended sediment concentration in an Eulerian frame, and this in turn leads to imbalances between the landward and seaward net sediment fluxes over a period of the fluid motion. When the settling and entrainment times are finite, but less than the timescale of the fluid motion, the process can be understood in terms of a particulate description of sediment behaviour; when the response is very rapid or is comparable to the hydrodynamic period, a continuum description is required.

The most robust result which our models reveal is a tendency for the landwards transport of sediment in very shallow water. However, it is misleading to think of this as arising from a single mechanism. For the simplest case, tidal flow on a linear flat, the mechanism is the difference in fluid depths, and thus in settling distances, following different fluid elements. For tidal flow on a convex flat, the dominant mechanism is the overall difference in fluid depth at HWS and LWS; in this case, however, settling lag plays a different rôle further from the shore, where the bathymetry encourages the export of sediment by shortening the duration of HWS.

The solutions for infragravity waves also illustrate the tendency of settling lag to import sediment into regions of generally lower velocities, which under some circumstances can promote the seawards movement of sediment. However, it is evident that this effect is rather weak, and easily overcome by the typical landwards flux in shallow water. This landwards flux is also powerful enough largely to overcome the effect of seawards-directed peak current velocities. However, if the sequence in which peak landwards and seawards flows occur is varied, this can have a significant effect on net transport. This illustrates the hysteresis involved in lag effects, which is a considerable pitfall for attempts to construct time-averaged models of advective sediment transport.

It is also instructive to compare figures 2 through 6. The differences between the hydrodynamics in these three cases are not pronounced, with fluid elements following a near-sinusoidal trajectory throughout the fluid motion; however, the patterns of net sediment transport are significantly different. In particular, it is interesting to note that even when the greatest differences in the hydrodynamics occur near the shoreline, the greatest differences in the sediment transport may occur in rather deeper water (compare figures 3b and 4b). This emphasises the non-local nature of advective sediment transport.

In summary, the model results described here suggest that settling lag is most accurately regarded not as a single mechanism but as an effect which may arise from, and be modified by, a wide range of hydrodynamic “asymmetries”. These effects do not necessarily work together, and do not necessarily lead to net landwards sediment transport; indeed, it may be possible in some circumstances for them largely to cancel out, leading to near morphodynamic equilibrium. Our results therefore warn against too simplistic an interpretation of lag effects in a coastal environment. However, by illustrating the connection between Lagrangian and Eulerian lag effects, the results suggest how observational data may be interpreted in these terms. This is of particular interest because recent field studies of intertidal flats (for example Christie *et al.* 1999; Bassoullet *et al.* 2000) have aimed to clarify the mechanisms of sediment transport by measuring or estimating the Eulerian cross-shore flux of suspended sediment, and our results suggest that, despite its subtleties, settling lag remains a useful paradigm for understanding many aspects of this process.

Figures

In all the figures, quantities shown are non-dimensionalised with regard to natural scales arising in the problem. For full details, see Pritchard & Hogg (2003a,b).

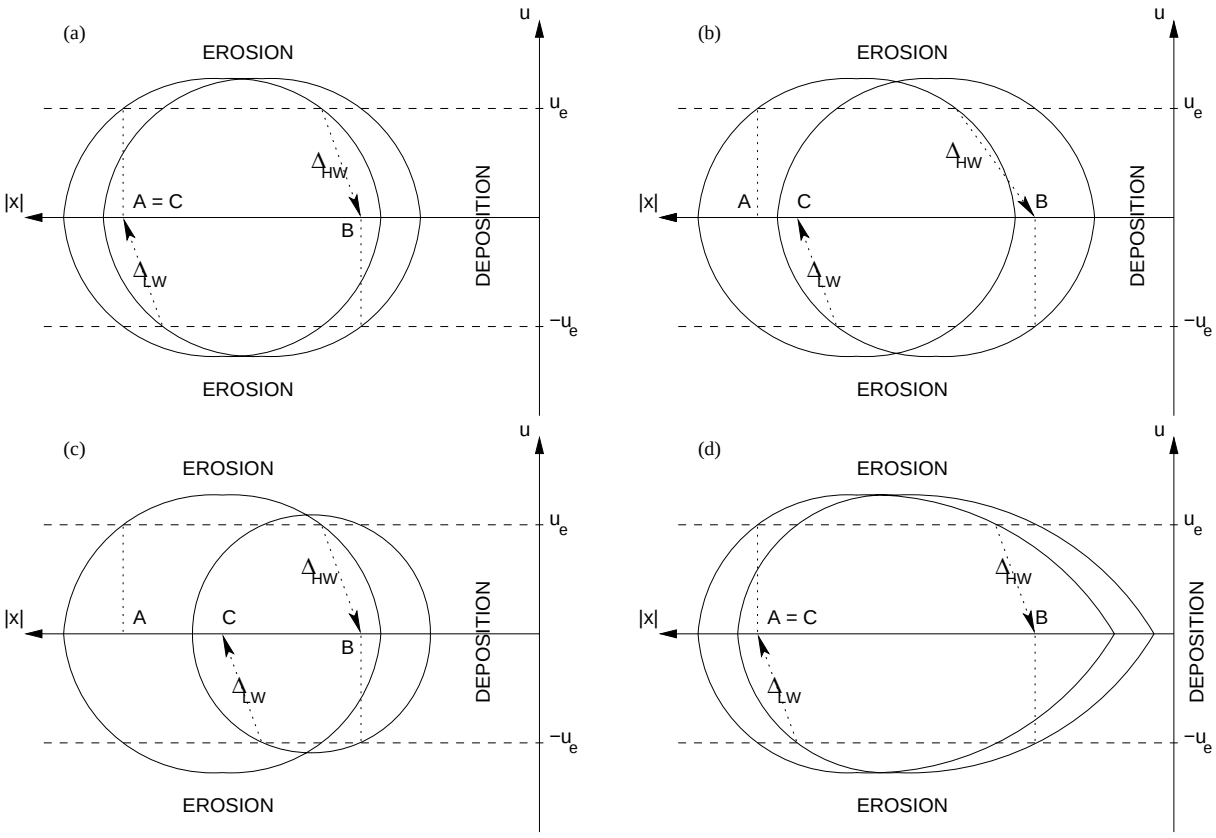

Figure 1: Schematics illustrating various causes of settling lag. Solid lines represent fluid trajectories; dashed lines represent $|u| = u_e = u_d$; dotted lines represent particle settling and re-entrainment.

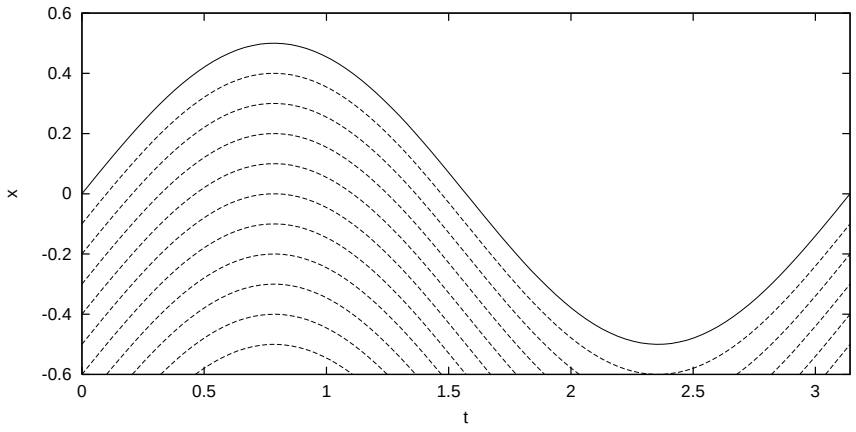

Figure 2: Fluid trajectories $x_L(t)$ under tidal flow across a linear flat. The solid line represents the shoreline; dashed lines represent successively more seawards fluid elements.

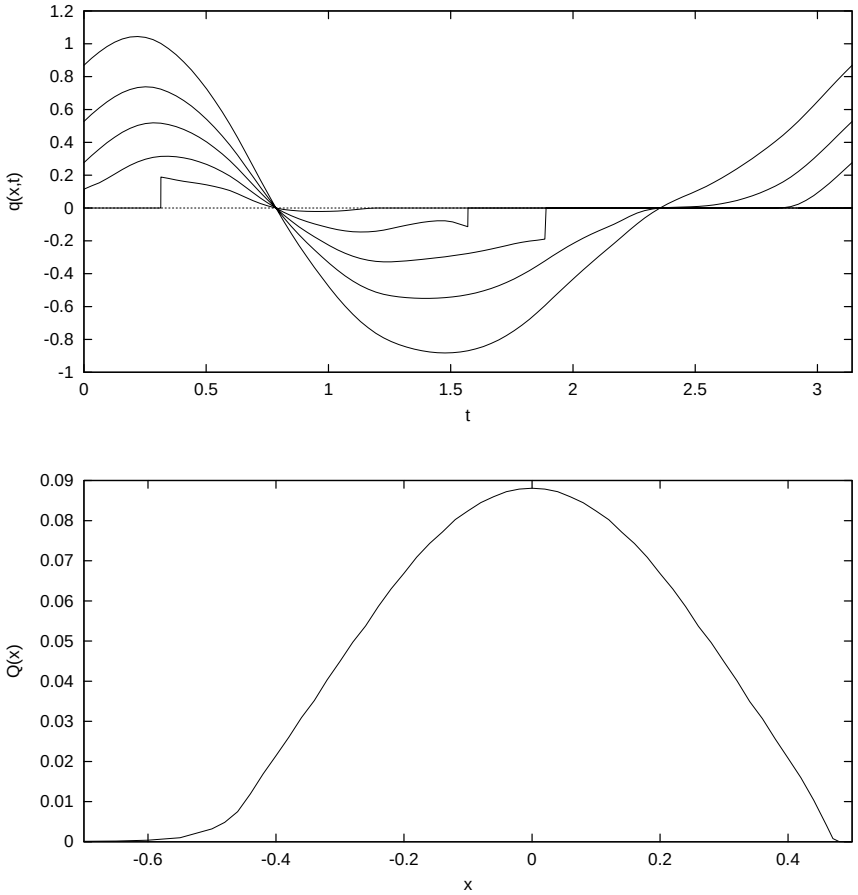

Figure 3. Instantaneous and net sediment flux across a linear flat under tidal currents. The upper plot shows sediment flux *q(x,t)* at various points across a linear flat under tidal currents; the lower plot shows the net sediment flux *Q(x)* over a tide.

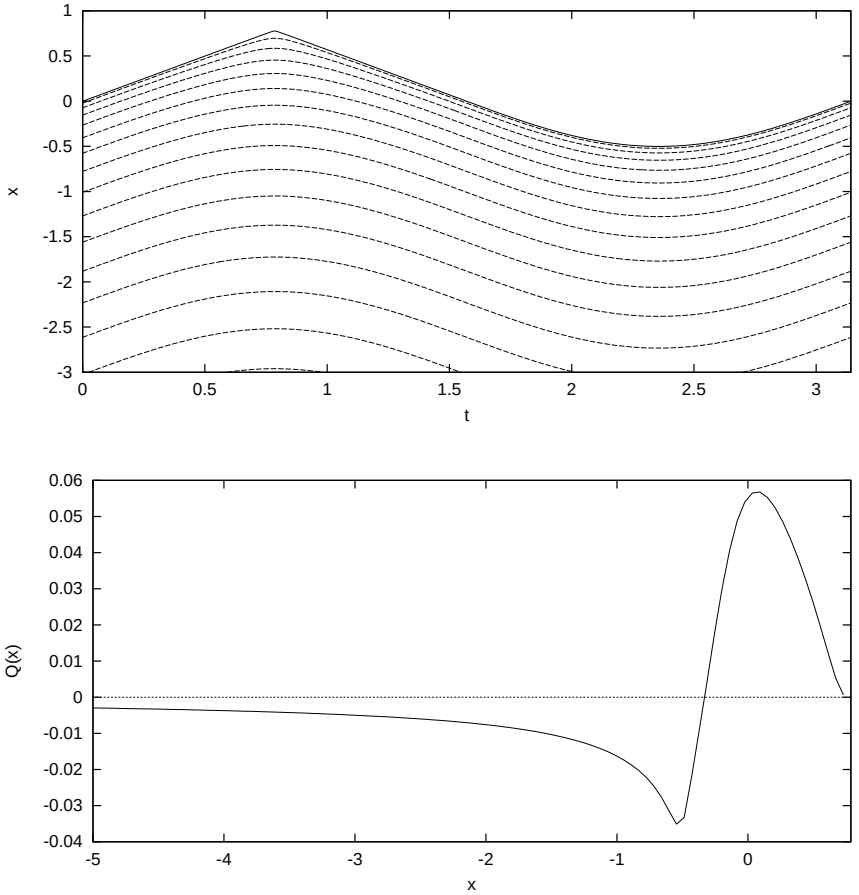

Figure 4. Hydrodynamics and net sediment flux across a linear-convex flat under tidal currents. The upper plot shows fluid trajectories $x_L(t)$ (shoreline is solid line; dashed lines are more seawards fluid elements); the lower plot shows the net sediment flux *Q(x)* over a tide.

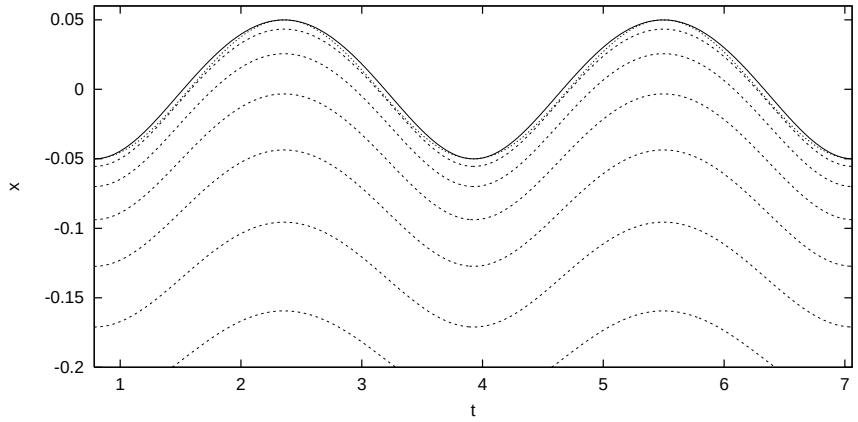

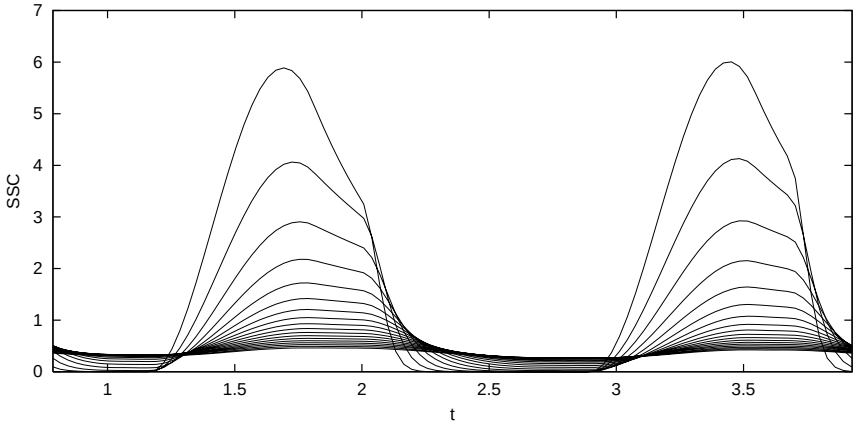

Figure 5. Hydrodynamics and sediment dynamics across a linear flat under a standing infragravity wave. The upper plot shows fluid trajectories $x_L(t)$ (shoreline is solid line and the dotted line represents a sinusoid; dashed lines are more seawards fluid elements); the lower plot shows SSC following various fluid elements behind the shoreline.

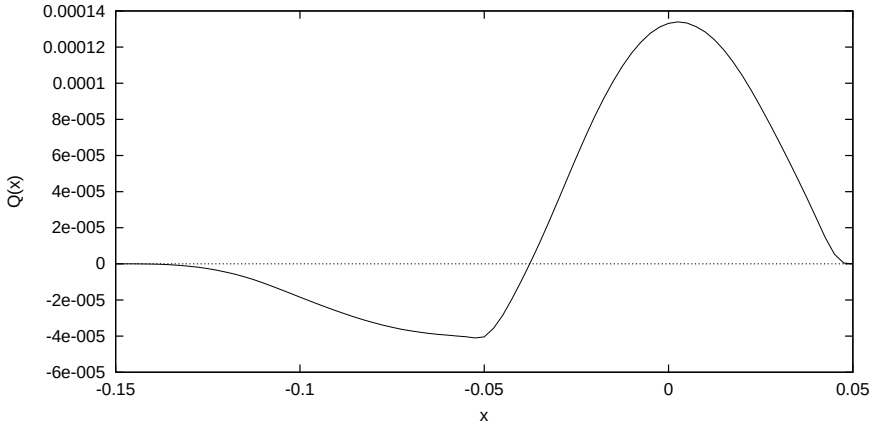

Figure 6: Net sediment flux *Q(x)* (integrated over a tide) across a linear flat under a standing infragravity wave.

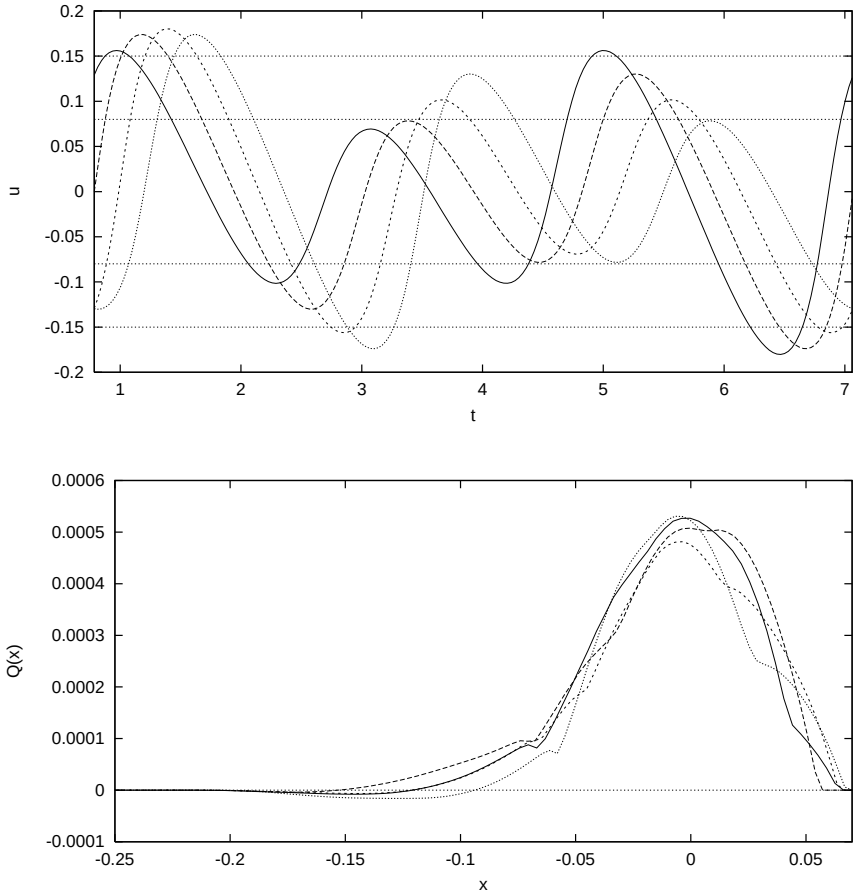

Figure 7: Hydrodynamics and net sediment flux across a linear flat under a bimodal infragravity wave. The upper plot shows the shoreline velocities for $\varphi = 0$ (solid), $\pi/4$ (dashed), $\pi/2$ (light dashed) and $3\pi/4$ (dotted); the lower point shows the corresponding net fluxes *Q(x)*.

References

Bassoullet, Ph. *et al.* 2000. Sediment transport over an intertidal mudflat. *Cont. Shelf Res.* **20**, 1635–1653.

Christie, M. C. *et al.* 1999. Sediment flux and bed level measurements from a macro-tidal mudflat. *Est., Coast. Shelf Sci.* **49**(5), 667–688.

Friedrichs, C. T. & Aubrey, D. G. 1996. Uniform bottom shear stress and equilibrium hypsometry of intertidal flats, 405–429 in C. Pattiaratchi (ed.), *Mixing in Estuaries and Coastal Seas* (AGU, Washington).

Groen, P. 1967. On the residual transport of suspended matter by an alternating tidal current. *Neth. J. Sea Res.* **3**, 564–574.

Postma, H. 1961. Transport and accumulation of suspended matter in the Dutch Wadden Sea. *Neth. J. Sea Res.* **1**, 148–190.

Pritchard, D. & Hogg, A. J. 2003a. Cross-shore sediment transport and the equilibrium morphology of mudflats under tidal currents. Under review.

Pritchard, D. & Hogg, A. J. 2003b. On fine sediment transport by long waves in the swash zone. Under review.

van Straaten, L. M. J. U. & Kuenen, P. H. 1958. Tidal action as a cause of clay accumulation. *J. Sed. Petrol.* **28**, 406–413.